NEAR-EXTINCTION AND FINAL BURNOUT IN COAL COMBUSTION

Robert H. Hurt* and Kevin A. Davis
Combustion Research Facility
Sandia National Laboratories, Livermore, CA 94550

* Author to whom correspondence should be addressed
TEL: (510) 294-3707
FAX: (510) 294-2276

The authors prefer an oral presentation and publication in the proceedings volume

E. Experimental Data and Interpretation;
D. Experimental Methodologies
(6.2) Coal and Organic Solids Combustion

Word count

body	3501 wds
nomenclature table	126 wds (18 lines x 7 wds/line)
references	336 wds (48 lines x 7 wds/line)
Acknowledgments	35 wds (5 lines x 7 wds/line)
Subtotal text	3998
Fig 1	200
Fig. 2	360 (across two columns)
Fig 3	450 (across two columns)
Fig 4	280 (across two columns)
Fig 5	200
Subtotal figures:	1490 wds
TOTAL	**5488 wds**

ABSTRACT

The late stages of char combustion have a special technological significance, as carbon conversions of 99% or greater are typically required for the economic operation of pulverized coal fired boilers. In the present article, two independent optical techniques are used to investigate near-extinction and final burnout phenomena for Illinois #6 and Pittsburgh #8 bituminous coals. Captive particle image sequences, combined with *in situ* optical measurements on entrained particles, provide dramatic illustration of the asymptotic nature of the char burnout process. Single particle combustion to complete burnout is seen to comprise two distinct stages: (1) a rapid high-temperature combustion stage, consuming about 70% of the char carbon and ending with near-extinction of the heterogeneous reactions due to a loss of global particle reactivity, and (2) a final burnout stage occurring slowly and at lower temperatures. For particles containing mineral matter, the second stage can be further subdivided into: (2a) late char combustion, which begins after the near-extinction event, and converts carbon-rich particles to mixed particle types at a lower temperature and a slower rate; and (2b) decarburization of ash — the removal of residual carbon inclusions from inorganic (ash) frameworks in the very late stages of combustion. This latter process can be extremely slow, requiring over an order of magnitude more time than the primary rapid combustion stage. For particles with very little ash, the loss of global reactivity leading to early near-extinction is clearly related to changes in the carbonaceous char matrix, which evolves over the course of combustion due to simultaneous oxidation and heat treatment. Current global kinetic models used for the prediction of char combustion rates and carbon burnout in boilers do not predict the asymptotic nature of char combustion. More realistic models accounting for the evolution of char structure are needed to make accurate predictions in the range of industrial interest.

INTRODUCTION

The late stages of char combustion have a special technological significance, as carbon conversions of 99% or greater are typically required for the economic operation of commercial-scale boilers. Achieving such high conversions is difficult in certain cases, especially in connection with boilers retrofitted with combustion zone modifications for NO_x abatement [1]. While there is an extensive literature on ignition [2], and char combustion [3-5], little attention has been paid to extinction in the important late stages of combustion, in part due to the difficulty of making scientifically meaningful measurements on highly reacted samples in which inorganic material (ash) is the majority constituent.

In the present article, two independent optical techniques are used to make kinetic measurements on complex highly-reacted samples with high inorganic content. The first technique uses *in situ* optical measurements on entrained char particles burning in a laminar flow reactor, coupled with a recently proposed criterion [6] for distinguishing inorganic from carbon-rich particles by measurement of their spectral emissive factors† in the near-infrared. After eliminating inorganic particles (which could otherwise masquerade as low-reactivity carbon-rich particles), conversion-dependent kinetic parameters are determined for the carbon-rich particles alone. The second technique uses a new captive-particle imaging apparatus equipped for simultaneous near-infrared thermography. This system is specifically designed for qualitative and quantitative investigation of the late stages of char combustion. The combination of these two techniques is used to investigate near-extinction and final burnout phenomena for Illinois #6 and Pittsburgh #8 bituminous coals. A goal of this work is to ascertain whether existing char combustion kinetics models can be extrapolated to high-conversion, or whether more detailed models of carbon burnout are needed that deal specifically with the chemical and physical phenomena unique to this region.

---

† The spectral emissive factor at 800 nm, ε_{800} for an irregularly-shaped, emitting particle, with a diameter along the flow axis of d_p, is defined as the average spectral radiance ($W/cm^2\ sr^{-1}\ \mu m^{-1}$) of the particle at a given wavelength (here 800 nm) divided by the spectral radiance of a spherical black body with diameter d_p. The spectral emissive factor is, in essence, the particle spectral emissivity multiplied by a shape factor, $A_p/(\pi d_p^2/4)$, where A_p is the projected area of the particle as viewed from the optical axis.

Previous work

A number of previous investigations of pulverized coal combustion have used single-particle imaging techniques, based on high-speed photography of entrained particles [7,8], holographic techniques [9], and CCD array detection [10]. Captive particle techniques have been used by various groups [11-13] for the study of coal devolatilization and combustion, with emphasis on swelling, morphological changes, and burnout times. These techniques have generated important insights, but none is designed specifically for quantitative investigation of the kinetics of extinction and final burnout for particles in the pulverized size range (< 200 μm). There is little information on extinction in coal combustion. Essenhigh [5] reports one study on flame extinction, and Ubhayakar et al. [14] have examined the thermal extinction of single graphite particles heated by a laser in cold surroundings

Although numerous papers report on the characterization of commercial or pilot-scale residues [15-17], few studies have focused on the late stages of char combustion under carefully controlled conditions. Among those, Nandi and Vleeskins [18] have investigated the fuel-related factors determining the degree of coal burnout in a drop tube furnace. Mitchell [19] observed numerous particles with low temperatures at high conversion, and has identified them as highly-reacted, high-inorganic-content char particles. A recent paper examined the low temperature particles in more detail [6], using an optical diagnostic to distinguish inorganic from carbon-rich particles by *in situ* measurement of their spectral emissive factors, ε_{800}, at a wavelength of 800 nm. It was found that a threshold value of 0.3 for the emissive factor could be used to statistically classify particles as carbon-rich ($\varepsilon_{800} > 0.3$) or inorganic ($\varepsilon_{800} < 0.3$) with an error rate or frequency of incorrect assignment of 4% or less. Application of the diagnostic indicates that most particles still contain substantial amounts of carbon at the point of abrupt temperature decrease, and that this residual carbon is oxidized slowly in a second, low-temperature combustion stage. In this work, near-extinction was defined as a large and abrupt, but mathematically continuous, decrease in particle temperature in the late stages of char combustion due to loss of global reactivity. The present paper continues the investigation of the late stages of combustion by acquiring data at longer residence times, by determining conversion-dependent kinetics, and by applying a new captive-particle imaging technique specifically designed to probe near-extinction and final burnout.

MATERIALS AND EXPERIMENTAL PROCEDURES

Illinois #6 (PSOC-1493D) and Pittsburgh #8 (PSOC-1451D) high-volatile bituminous coals were chosen for this investigation. The two independent combustion experiments, involving entrained and captive particles respectively, are described separately below. Figure 1 depicts the captive particle imaging (CPI) apparatus. Char particles of 50 - 300 μm in diameter† are placed on a low-density particle support and inserted into the flow reactor through a open test section in the quartz wall (see Fig. 1). The support is surrounded by a small conical cooling coil which maintains the particle at 200 - 300 °C, while it is brought into the focal volume of a modified long-focal-length microscope. The cooling coil is then retracted, the particle is rapidly heated by the surrounding gases, and its ignition, combustion, and burnout behavior is imaged at high resolution using both reflected visible light and emitted light in the near infrared.

Because transport processes for particles in the pulverized size range are dominated by diffusion, conduction, and radiation, and not by convection [3], a mechanical suspension technique, if properly designed, will accurately simulate char combustion in entrained flows. (Note that convection does play a role in the combustion of larger particles, and in other combustion subprocesses such as devolatilization.) For pulverized char combustion studies, the suspension device can be allowed to perturb the flow field and thus the convective processes, if it does not present a significant barrier to diffusion, conduction, or radiation to and from the particle. The particle support used consists of a platinum ring, spanned in several places by 75 μm diameter platinum wires that provide support for a thin layer of fine (5 μm diameter) Al_2O_3 fibers (99% pure). Quantitative estimates [20] indicate that the low-solid-volume fraction of the fiber bed provides an environment in which the gas-to-particle mass and heat transfer coefficients are very similar to those for entrained particles. The flow field and the temperature transients at the beginning of the experiment have been characterized and are discussed in detail elsewhere [20]. Maximum heating rates are approximately $2 \cdot 10^3$ K/sec with good shot-to-shot reproducibility. The rapid and reproducible temperature transients combined with the avoidance of transients in gas composition make this flow configuration useful for investigating char combustion and burnout phenomena.

---

† Char samples were generated previously by injection of raw coal into a 1600 K gas stream in the laminar flow reactor and extraction of samples after 47 msec residence time.

The optical system comprises a long-focal-length microscope (model K2 of Infinity Photo-Optical) modified by addition of an internal beam splitter to allow simultaneous dual video imaging of the same field-of-view. Two CCD cameras record one image formed by reflected visible light (supplied by fiber-optic illumination) and a second formed by near-infrared emission from the particle surfaces. The near-infrared emission (700 - 1000 μm in wavelength) is selectively imaged by incorporating an optical filter in the quadrocular head, while reflected radiation in the same wavelength band is rejected by placement of an infrared filter within the fiber optic illuminator. The fiber-optic illumination is rejected so successfully, that this second optical channel records no image whatsoever until the particles reach approximately 900 K and begin to emit significantly in the near-infrared. The near-infrared channel has been calibrated with a high-temperature black-body source and the thermographic images are digitized and quantitatively analyzed to determine particle radiance temperatures.

In the second independent experiment, optical measurements were made of particle size, temperature, and emissive factor during combustion of dilute streams of entrained particles in a laminar flow reactor described elsewhere [19]. Residence times greater than 117 msec were obtained by rapid quenching and collection of solid samples followed by reinjection and further combustion. The collection and reinjection process has been shown to have no effect on the subsequent kinetics for single particles, although it may change the size distribution of the bulk sample by inducing fragmentation and/or reagglomeration of fines during collection and handling [21]. Because particle sizes are measured *in situ*, single-particle kinetics can be determined from the optical data with no errors introduced by the reinjection procedure. Total ash was used as a tracer to put determine carbon conversions for the bulk samples, and the weight loss at 47 msec residence time (where the visible volatiles flame disappears) was used to put the conversions on a volatile-matter-free, or char, basis.

RESULTS

Captive particle imaging

Image sequences were obtained for approximately one-hundred particles of Illinois #6 and Pittsburgh #8 coal chars, which exhibit statistical particle-to-particle variations in size, morphology and ash content. Figure 2 is a single-camera sequence illustrating the typical combustion behavior of particles of high mineral content. Shortly after retraction of the

cooling coil, a bright red optical emission from the solid surfaces becomes evident (see image at 0.12 sec in Fig. 2), indicating an elevated particle temperature. The bright incandescence lasts for about one-half second before it fades, indicating a significant decrease in particle temperature. Note that the temperature decrease occurs under nearly isothermal conditions in the gas phase (the local gas temperature is actually *increasing* slightly), and while the char particle still contains much visible dark material, typically elemental carbon.†

After the temperature decrease, combustion continues, slowly converting the carbon-rich particles to mixed particle types containing elemental carbon in their cores, or as islands within a coherent inorganic matrix. The final stage of the combustion process consists of the removal of these elemental carbon inclusions from a predominately inorganic matrix. This process, which we refer to here as "ash decarburization" can be extremely slow, requiring 10 - 30 seconds for the particle represented in Fig. 2. Another unique characteristic of high-mineral-content particles is that their combustion and burnout generally occurs without dramatic changes in the particle morphology or size. The mineral matter provides a cohesive framework from which elemental carbon is removed while preserving much of the original particle shape. No fragmentation, or structural rearrangement of the particles is typically observed. The ash frameworks, however, are often observed to slowly consolidate and densify after most of the carbon disappears, due perhaps to sintering mechanisms.

The low-mineral-content, low-density particles, in contrast, undergo profound morphological changes during combustion. Consumption of carbon from these particles often results in loosely connected, fragile structures at moderate to high conversion. Such particles are much more likely to fragment during combustion, but instead of producing distinct fragments, they are typically observed to contract or reagglomerate to yield a single ash particle. Further work is needed to understand the contraction process and its implications for particle fragmentation. It is particularly noteworthy that particles of very low mineral content also exhibit a brief period of bright incandescence followed by a distinct decrease in emission before the particle size and morphology change dramatically.

---

† Most, but not all, of the black material observed in these highly-reacted samples is elemental carbon, the remainder being primarily iron-bearing phases, as determined by laser spark spectroscopy.

To explore the near-extinction phenomenon in greater detail, dual images of reflected visible light and near-infrared emission were obtained for selected particles. An example dual image sequence is shown in Fig. 3, along with time-resolved radiance temperatures† determined from digitization of the near-infrared images. The combined data and images show a period of bright incandescence from 0.8 to 1.2 seconds, followed by a relatively abrupt drop in temperature of 125 K and a long, slow, nearly-isothermal, final burnout to a carbon-free ash particle. The gradual decrease in radiance temperature at long times is in part due to decreases in emissivity, but the initial rapid decrease reflects a decrease in actual temperature, since it is large, and occurs abruptly while the particles are still optically black. These data are particularly useful for defining the point of near-extinction—it occurs (1) when the local gas temperature is nearly constant or increasing slightly, (2) when the particle diameter is 85% of the initial diameter, (3) while the particle is still dark under visible illumination, before the appearance of visible surface ash. This near-extinction is observed even for particles containing very small amounts of mineral matter (as inferred from the size of the final ash particle). For these low-ash particles, the near-extinction is clearly not caused by the formation of an ash-film diffusion barrier.

In situ optical measurements on entrained particles

The second independent experiment produced a set of single-particle size, temperature, and emissive factor measurements for Illinois #6 coal char at various residence times. These data indicate a gradual transition from a population of fully ignited char particles at 72 ms to a predominance of low-temperature particles at 117 ms and, finally, to a predominance of inorganic-rich particles (with emissive factors < 0.3) at 306 ms. Figure 4 shows the time evolution of the particle temperatures and sizes for a subset of this raw data with emissive factors greater than 0.3 (representing the carbon-rich particles and mixed particle types [6]). The temperatures in Fig. 4 have been normalized by subtracting the local gas temperature, which changes slightly along the reactor length, to facilitate comparison among data at

---

† Radiance temperature is defined as the temperature of a hypothetical black body emitting the same radiative power as the real object (particle) in the wavelength range of interest (here 700 - 1000 nm). For carbon-rich particles such as those found up to about 2 sec in Fig. 4, whose emissivities are approximately 0.8 [22], true particle temperatures will be approximately 20 K greater than the reported radiance temperatures. The true temperatures of inorganic-rich and mixed particles are difficult to estimate due to the unknown and variable optical properties of ash on a particle-by-particle basis.

different residence times. The temperature *difference*, as plotted in Fig. 4, is a convenient indicator of the reaction rate at any point. Also shown on Fig. 4 are the theoretical temperature limits for diffusion-limited burning and for inert particles, calculated for various assumptions (see Fig. 4 caption).

Figure 4 clearly shows a large temperature drop or near-extinction occurring between 72 ms (69% bulk conversion) and 117 ms (75% bulk conversion). At 117 ms and beyond, a large group of particles is observed at or near the gas temperature, with a smaller but significant group having temperatures from 50 to 300 K above that of the gas. A small number of particles (approximately 10 of 184, or 6%) are still seen at the high temperatures associated with the rapid combustion phase. Different particles undergo near-extinction and final burnout at different times due to differences in particle density, reactivity [6], and initial ash content [19].

Conversion-dependent reactivities

Figure 5 presents global char reactivities at various conversions in the form of preexponential factors, A, extracted from the optical data using a model of gas-particle transport processes [23]. For this calculation, global kinetic parameters previously determined for Illinois #6 coal in the early-to-intermediate stages of combustion [23] were adopted† and the preexponential factor adjusted with conversion to match the mean measured particle temperature for the mean particle size. The reactivity in Fig. 5 decreases monotonically during combustion, dropping by a factor of 5 at 90% conversion. Conversion-dependent char reactivities have been previously observed under other conditions — see for example Hecker et al. [24]. The dashed line in Fig. 5 represents the assumption on which global kinetic models are typically based — a constant, conversion-independent global reactivity. The global kinetic model assumption does not lead to large errors below 50% conversion, but, by 70% conversion, the reactivity has decreased by a factor of about 2 and numerous near-extinction events are observed (see Fig. 4).

---

† The global parameters are a reaction order of 0.5, and activation energy of 22.5 kcal/mole, and a CO/CO_2 ratio given by $CO/CO_2 = 3.10^8 e^{(60/RTp)}$ with R in kcal/mol-K and T_p in K. Varying the assumed values of the reaction order, activation energy, and CO/CO_2 ratio was observed to have some effect on the reactivities, but not the basic downward trend in Fig. 5. The loss of reactivity with conversion is a gross effect for this system that is related to changes in the solid fuel properties and not to the form or details of the rate expression.

DISCUSSION AND CONCLUSIONS

The combination of *in situ* optical measurements and independent captive particle image sequences provide dramatic illustration of the asymptotic nature of the char burnout process. Single particle combustion to complete burnout comprises two distinct stages: (1) a rapid high-temperature combustion stage, consuming approximately 70% of the char carbon and ending with near-extinction of the heterogeneous reactions due to loss of global particle reactivity, and (2) a final burnout stage occurring slowly and at lower temperatures. For particles containing mineral matter, the second stage can be further subdivided into: (2a) late char combustion, which begins after a near-extinction event, and converts carbon-rich particles to mixed particle types at a lower temperature and a slower rate; and (2b) decarburization of ash — the removal of residual carbon inclusions from inorganic (ash) frameworks in the very late stages of combustion. This latter process can be extremely slow, requiring over an order of magnitude more time than the primary rapid combustion stage.

To understand the origin of the low reactivities, consider the classical Thiele theory of gas-solid reactions, where the overall particle burning rate, q, in zone II scales with char properties as $q \sim (\rho_c)^{1/2} (S)^{1/2} (k_i)^{1/2} (D_{eff}).^{1/2}$ Here ρ_c is the mass of carbon per unit particle volume, S is the internal surface per gram of carbon, k_i is the intrinsic reactivity of that surface, and D_{eff} is the effective diffusion coefficient in the porous particle. In general, the combustion process, which consists of oxidative carbon removal and simultaneous high temperature heat treatment [25], can alter each of these parameters: ρ_c [5], k_i [24], A [26], and D_{eff} [27]. The low global reactivities (expressed per unit external particle area) during ash decarburization are not surprising, as the inorganic matter displaces carbon leading to a low value of ρ_c and can also act as a diffusion barrier (low D_{eff}). This carbon depletion effect alone will produce low global reactivities at very high burnout for ash-containing particles.

A more significant observation is the initial temperature drop, that we refer to as a near-extinction event, which is exhibited by most of the particles investigated. The near-

extinction is caused by a loss of global reactivity†, and occurs for both high and very low ash content particles, often before ash becomes visible on the particle surfaces. For particles with very little ash, the loss of global reactivity is clearly related to changes in the carbonaceous phase, rather than interactions with the bulk mineral matter.†† Because coal chars are microporous carbons, k_i, A, and D_{eff} are all strongly influenced by the crystallinity and ultrafine structure of the carbonaceous matrix. In a concurrent paper, Davis et al. [28] demonstrate that the carbon crystalline structure evolves dramatically over the course of the combustion process under the conditions of interest here.

The asymptotic nature of the char combustion process has important implications for the modeling of carbon burnout in furnaces. Current global models typically used assume a reactivity that is independent of conversion and consequently predict high particle temperatures and rapid heterogeneous combustion rates until the solid fuel is completely consumed. This simplified approach leads to a systematic error—carbon persists well beyond the point at which global kinetic models predict complete burnout. More realistic conversion-dependent models are needed to make accurate predictions in the range of industrial interest.

ACKNOWLEDGMENTS

Financial support for this work is provided by the U.S. DOE Pittsburgh Energy Technology Center's Direct Utilization Advanced Research and Technology Development Program. The technical contributions of James Ross, Richard Yee, C. Scott Kelley, Carlos Gethers, and F. William Kent are gratefully acknowledged.

---

† Particle temperature depends upon particle size through equations describing mass and energy transport, and spontaneous thermal extinction has been observed under some conditions [14] as particle size decreases during combustion at constant reactivity. This is not the mechanism involved in the present study, however. Calculations performed for both sets of conditions (in the CPI and entrained flow experiments) indicate that decreases in particle size at constant reactivity cannot explain the observed near-extinction events. The magnitude of the temperature drop (and burning rate decrease) during near-extinction is a function its surroundings; it is larger at high oxygen levels and low gas temperatures, but the underlying cause is the same—a loss of global reactivity.

†† Note that the carbonaceous phase is defined here to include small quantities of finally-dispersed mineral matter, if any, which may increase the intrinsic reactivity of carbon surfaces through catalysis.

NOMENCLATURE

A	global reactivity, g-carbon cm^{-2} s^{-1} atm^{-n} (cm^{-2} of external area)
A_p	projected area of a char particle along the optical axis
D_{eff}	effective diffusivity, cm^2 s^{-1}
d_p	particle diameter, cm
k_i	intrinsic reactivity, g-carbon cm^{-2} s atm (cm^{-2} of total area)
R	gas constant, kcal $mole^{-1}$ K^{-1}
q	overall particle burning rate, g-carbon cm^{-2} s^{-1} (cm^{-2} of external area)
t	time, s
S	total surface area, m^2 g^{-1}
T_g	gas temperature, K
T_p	particle temperature, K
X	char carbon conversion, volatile-matter-free basis

Greek symbols

ε	total emissivity, or emissivity
ε_{800}	spectral emissive factor at 800 nm, or "emissive factor"
λ	radiation wavelength, nm
ρ_c	mass of carbon per unit particle volume, g cm^{-3}

REFERENCES

1. Fiveland, W. A., and Jamaluddin, A. S., *Combust. Sci. and Tech.*, 81:147-167 (1992).

2. Essenhigh, R. H., Misra, M. K., and Shaw, D. W., *Comb. and Flame* 77:3-30 (1989).

3. Field, M. A., *Combustion and Flame* 14:237-252 (1970).

4. Smith I. W., *Nineteenth Symposium (International) on Combustion*, The Combustion Institute, Pittsburgh, 1982, pp. 1045-1065.

5. Essenhigh, R. H., in *Chemistry of Coal Utilization, Second Supplementary Volume* (M.A. Elliot, Ed.) John Wiley and Sons, New York, 1981, p. 1153.

6. Hurt, R. H. "Reactivity Distributions and Extinction Phenomena in Coal Combustion" to appear in *Energy and Fuels* (1993).

7. McLean, W. J., Hardesty, D. R., and Pohl, J. H., *Eighteenth Symposium (International) on Combustion*, The Combustion Institute, Pittsburgh, 1981, pp. 1239 - 1248.

8. Timothy L. D., Froelich, D., Sarofim, A. F., and Beer, J. M. *Twenty-First (International) Symposium on Combustion*, The Combustion Institute, Pittsburgh, 1986, pp. 1141 - 1148.

9. Seeker, W. R., Samuelsen, G. S., Heap, M. P., and Trolinger, J. D. *Eighteenth (International) Symposium on Combustion*, The Combustion Institute, Pittsburgh, 1981, pp. 1213-1226.

10. Schroeder, A. R., Thompson, D. M., Daves, G. G., Buckius, R. O., Krier, H., and Peters, J. E. *Twenty-Fourth (International) Symposium on Combustion*, The Combustion Institute, Pittsburgh, 1992, pp. 1161 - 1169.

11. Essenhigh, R. H., and Yorke, G. C., *Fuel* 44:177-186 (1965).

12. Shibaoka, M., *J. Inst. Fuel* 42:59-66 (1969).

13. Thomas, C. G., Shibaoka, M., Gawronski, E., Gosnell, M. E., Brunckhorst, L. F., and Phong-anant, D. *Fuel* 72(7):907-912 (1993).

14. Ubhayakar, S. K., and Williams, F. A., *J. Electrochemical Soc.* 123:747-756 (1976).

15. Walsh, P. M., Xie, J., Douglas, R. E., Battista, J. J., and Zawadzki, E. A. "Unburned Carbon Loss from Pulverized Coal Combustion," submitted to Fuel (1993).

16. Nandi, B. N., Brown, T. D., and Lee, G. K., *Fuel* 56 125 (1977).

17. Shibaoka, M. *Fuel* 64:263-269 (1985).

18. Vleeskens, J. M. and Nandi, B. N., *Fuel* 65 797-802 (1986).

19. Mitchell, R. E. *Twenty-Third (International) Symposium on Combustion*, The Combustion Institute, Pittsburgh, 1990, pp. 1297 - 1304.

20. Hurt, R. H., Davis, K. A., and Hardesty, D. R. in *Coal Combustion Science--Quarterly Progress Report,* Sandia Technical Report, July - September, 1993.

21. Hurt, R. H., Davis, K. A., and Hardesty, D. R. in *Coal Combustion Science--Quarterly Progress Report,* Sandia Technical Report, January - March, 1993.

22. Baxter, L. L., Fletcher, T. H., and Ottesen, D. K., *Energy and Fuels* 2:423-430 (1988).

23. Hurt, R. H., and Mitchell, R. E., *Twenty-Fourth(International) Symposium on Combustion,* The Combustion Institute, Pittsburgh, 1992, pp. 1243 - 1250.

24. Hecker, W. C., McDonald, K. M., Reade, W., Swensen, M. R., and Cope, R. F. *Twenty-Fourth (International) Symposium on Combustion*, The Combustion Institute, Pittsburgh, 1992, pp. 1225-1231.

25. Suuberg, E. M. in *Fundamental Issues in Control of Carbon Gasification Reactivity*, Kluwer Academic Publishers, 1991, pp. 269-305.

26. Smith, I. W., and Tyler, R. J., *Fuel* 51:312-321 (1972).

27. Mitchell, R. E., and Tsai, N. K., *International Conference on Coal Science Proceedings*, 1993, Vol. 1, pp. 19-22.

28. Davis, K. A., Hurt, R. H., Yang, N. Y. C., and Headley, T. H., "Evolution of Char Chemistry, Crystallinity, and Ultrafine Structure during Pulverized Coal Combustion," submitted to the *Twenty-Fifth (International) Symposium on Combustion,* 1993.

FIGURE CAPTIONS

Figure 1. Schematic of the captive particle imaging apparatus. Analog and digital image acquisition, storage, and processing hardware is not shown.

Figure 2. Single camera captive particle image sequence for a typical Illinois #6 coal char particle. Combustion of ≈150 μm particle in 6 mole-% oxygen at a steady-state local gas temperature of 1360 K. Images formed by reflected visible light. Images and timeline show the duration of the rapid, incandescent combustion phase and the lower temperature final burnout phase.

Figure 3. Dual camera captive particle image sequence for typical Illinois #6 coal char particle. Combustion of ≈200 μm particle in 6 mole-% oxygen at a steady-state local gas temperature of 1250 K. Zero time is defined as the point of first visible incandescence, which corresponds to a particle temperature of approximately 900 K.

Figure 4. Optical measurements of particle size and normalized particle temperature for combustion of Illinois #6 coal in 12 mole-% oxygen. Points represent carbon-rich particles with emissive factors greater than 0.3. The number of low-emissive-factor particles excluded from Fig. 4 increases from 8 of 184 (4 % of the total) at 117 msec to 151 of 241 (63% of the total) at 309 msec. Curves at high-temperature represent diffusion-limits for two assumptions regarding the product ratio: dashed line for CO/CO_2 molar ratio given by $3x10^8\ E^{(-60/RT_p)}$ with RT_p in kcal/mol [23]; Dot and dash pattern for CO as sole reaction product. Curves at low temperature are temperature limits for inert particles with varying total emissivities: dashed line for $\varepsilon = 0.8$, dot and dash pattern for $\varepsilon = 0.4$.

Figure 5. Effect of carbon conversion on the reactivity of carbon-rich particles of Illinois #6 coal char. Combustion in 12 mole-% oxygen for residence times from 72 to 306 msec. Particles with emissive factors less than 0.3 (inorganic-rich particles) were excluded prior to analysis. Triangles—measured reactivities; Solid line—fitted curve; Dashed line—global kinetic model of Hurt and Mitchell [23], presented for comparison.

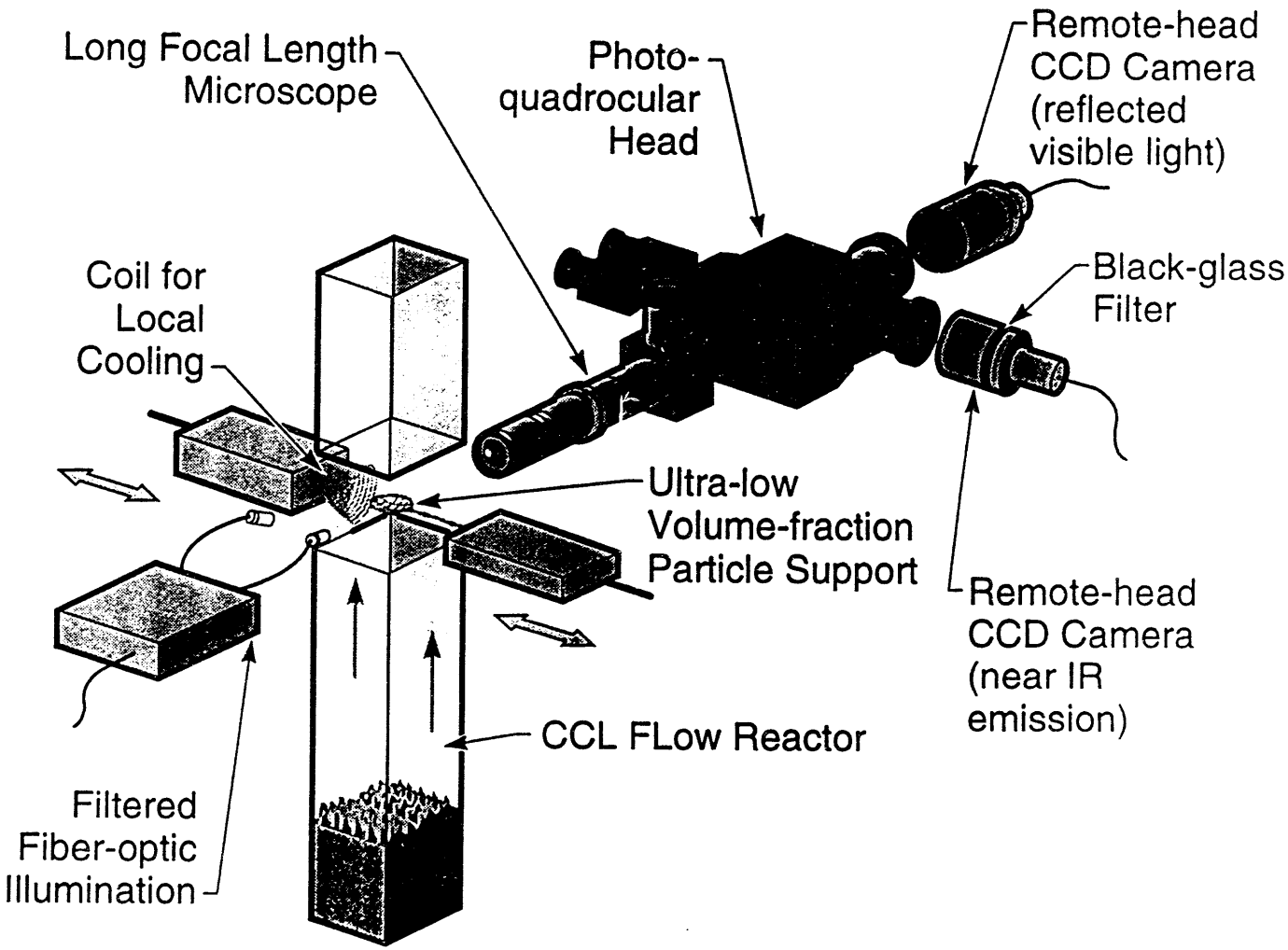
Long Focal Length Microscope
Photo-quadrocular Head
Remote-head CCD Camera (reflected visible light)
Black-glass Filter
Coil for Local Cooling
Ultra-low Volume-fraction Particle Support
Remote-head CCD Camera (near IR emission)
CCL FLow Reactor
Filtered Fiber-optic Illumination

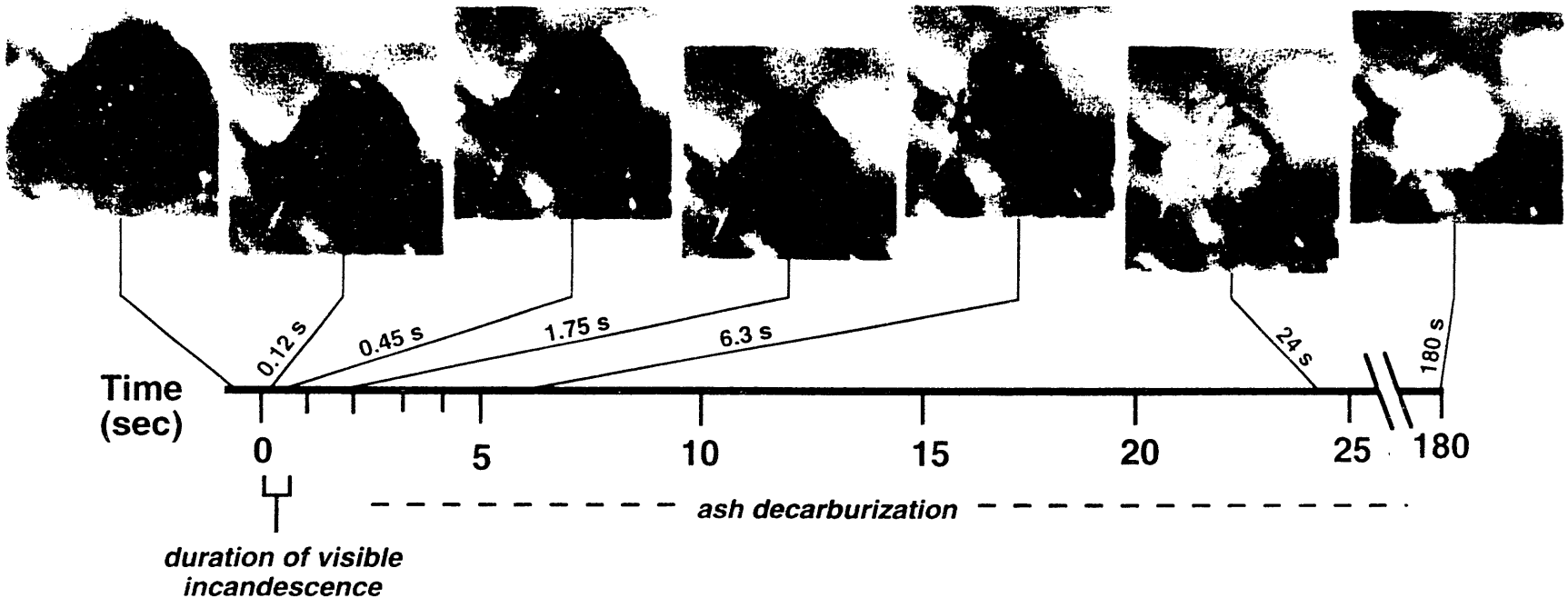
0.12 s
0.45 s
1.75 s
6.3 s
24 s
180 s
Time
(sec)
0
5
10
15
20
25
180
ash decarburization
duration of visible
incandescence

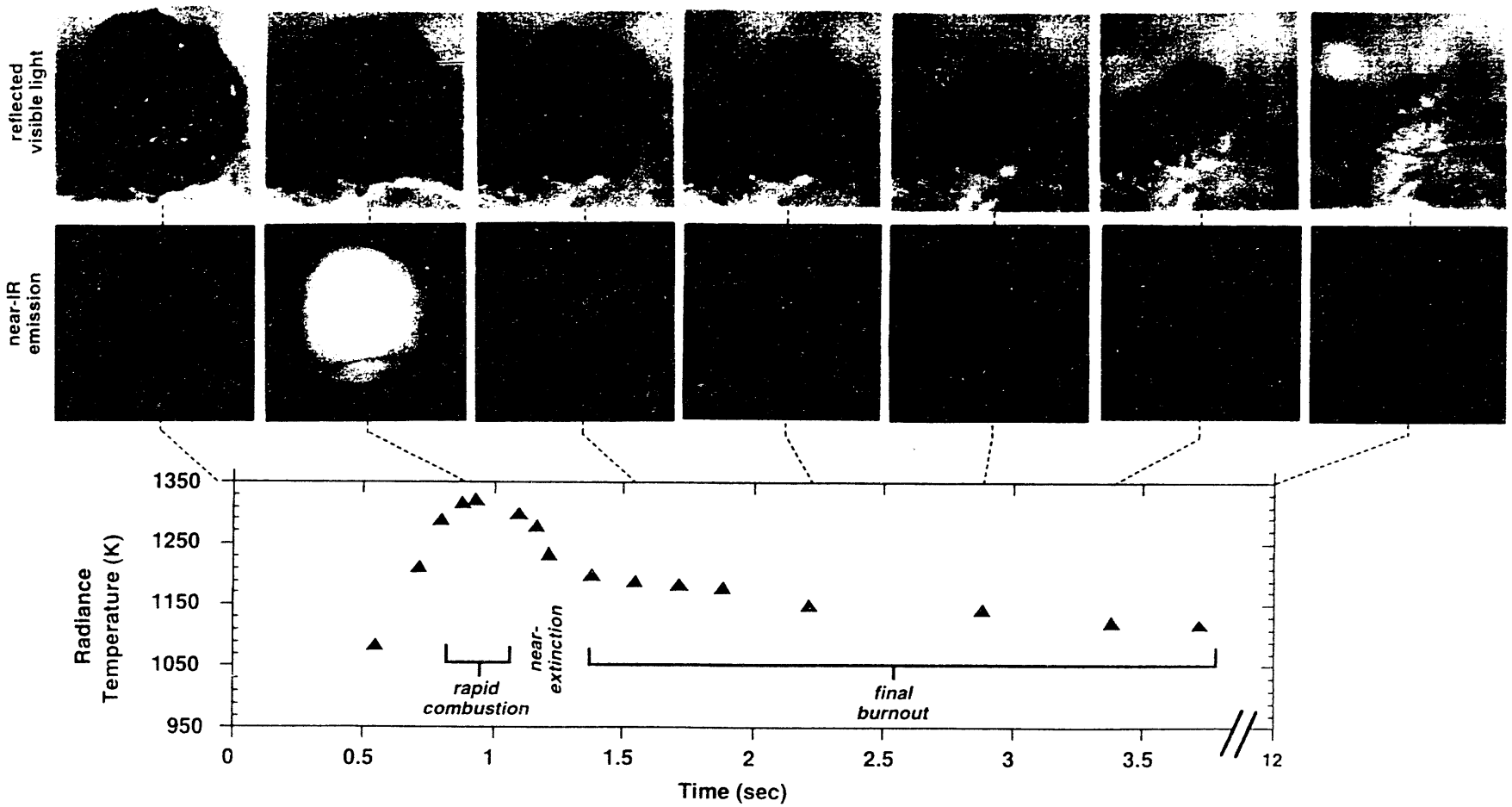
reflected visible light
near-IR emission
Radiance Temperature (K)
1350
1250
1150
1050
950
0
0.5
1
1.5
2
2.5
3
3.5
12
Time (sec)
rapid combustion
near-extinction
final burnout

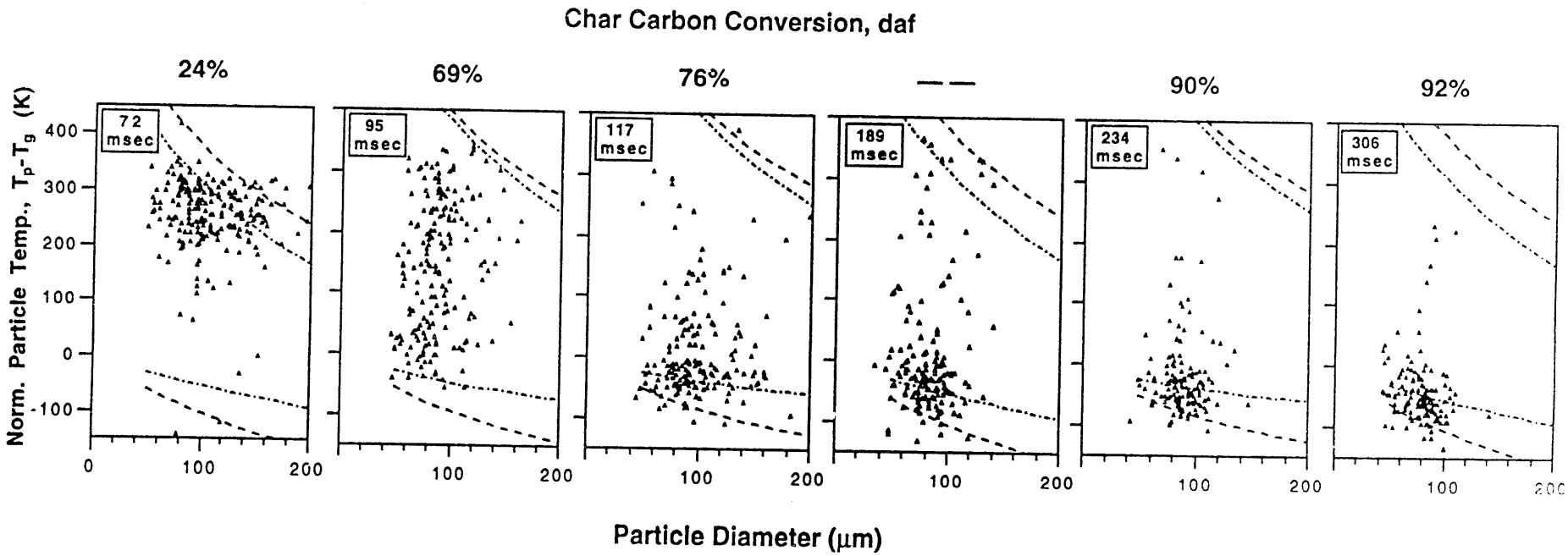
Char Carbon Conversion, daf
24%
69%
76%
90%
92%
72 msec
95 msec
117 msec
189 msec
234 msec
306 msec
Norm. Particle Temp., T_p-T_g (K)
400
300
200
100
0
-100
0
100
200
Particle Diameter (μm)

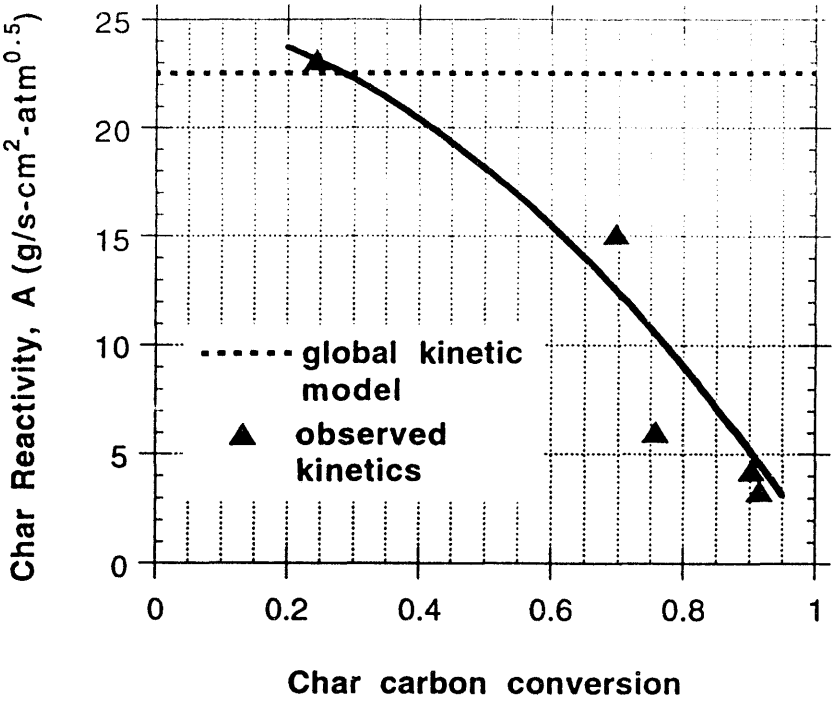
Char Reactivity, A (g/s-cm^2-atm$^{0.5}$)
25
20
15
10
5
0
0
0.2
0.4
0.6
0.8
1
global kinetic model
observed kinetics
Char carbon conversion

DATE
FILMED
6/3/94
END